Mechanics and Mechanical Engineering
Vol. 15, No. 1 (2011) 61–72

The Strength of Cut–off Wheel Model Subjected to a Single Point Lateral Load Assessed by Different Methods

Józef Kaczmarek
Department of Production Engineering
Technical University of Łodz
Stefanowskiego 1/15, 90–924 Łodz, Poland

Jacek Świniarski
Department of Strength of Materials and Structures
Technical University of Łodz
Stefanowskiego 1/15, 90–924 Łodz, Poland

Received (13 November 2010)
Revised (15 January 2011)
Accepted (25 April 2011)

In the paper the estimation results of strength of a cut–off wheel model subjected to a single point lateral load in the form of a reduced stress obtained by three methods: analytical, FEM (finite–element method) and strain gauge method have been presented. The applicability of the particular methods has also been discussed.

Keywords: Cut–off wheel model, single point lateral load, strength, different methods

1. Introduction

Cut–off wheels are among the most commonly used grinding wheels. They are used by a variety of industrial manufacturing plants as well as by individual users. These tools work in rugged loading conditions, including: the centrifugal force load resulting from a high machining speed (at present: $80 \div 100$ m/s) and lateral loads, which can occur while cutting objects of complicated shapes, differently located with respect to the cut–off wheel, and while cutting by means of manual cut–off machines. The insufficient strength of a cut–off wheel can cause its tear while running, which can be very dangerous for abrasive cut–off machines. For this reason, nowadays many researchers and manufacturers of cut–off wheels devote much time to researching the cut–off wheel strength. One of many methods of the cut–off wheel strength testing [1] is a method consisting in the tangential use of a single point lateral load located near the circumference of the cut–off wheel. The cut–off wheel does not rotate during this investigation. The method is characterized by

kinematics simplicity and a low cost of the investigation stand. Such stands can even be used by small plants manufacturing cut–off wheels.

2. Cut–off wheel model and its loading scheme

Cut–off wheel model consists of thin circular plate which is single point loaded on circumference by lateral load F. It is shown schematically in Fig. 1, however loading of cut–off wheel sector is depicted in Fig. 2.

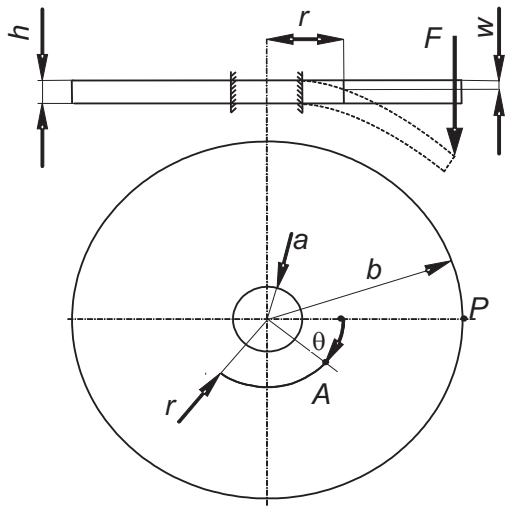

Figure 1 Scheme of support and a single point load of cut–off wheel: a – radius of fastening (of fixing discs) of cut–off wheel, b – external radius of cut–off wheel, F – lateral load put against cut–off wheel (from press down disc)

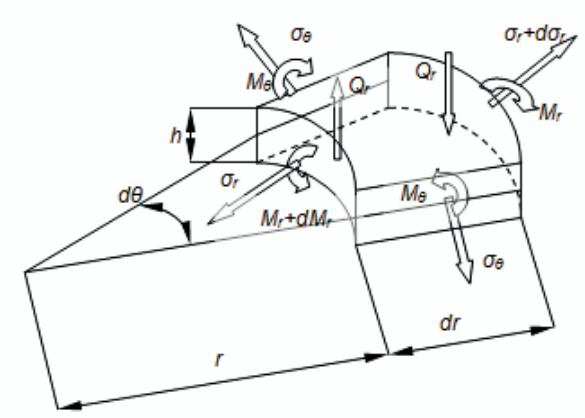

Figure 2 Loading scheme of cut–off wheel sector for single point test

3. Analytical method of stresses estimation in accepted cut–off wheel model

Differential equation of deflection loaded surface of circular plate is equal to [5]:

$$\left(\frac{\partial^2}{\partial r^2}+\frac{1}{r}\frac{\partial}{\partial r}+\frac{1}{r^2}\frac{\partial^2}{\partial\theta^2}\right)\left(\frac{\partial^2 w}{\partial r^2}+\frac{1}{r}\frac{\partial w}{\partial r}+\frac{1}{r^2}\frac{\partial^2 w}{\partial\theta^2}\right)=\frac{Q}{D} \tag{1}$$

where:

Q – plate loading in general depiction

D – plate stiffness expressed by the equation [3, 4, 5]:

$$D=\frac{Eh^3}{12(1-\nu^2)} \tag{2}$$

where:

E –Young's modulus,

h – cut–off wheel thickness,

ν – Poisson number of cut–off wheel material.

Uniform equation of deflection loaded surface of circular plate is defined by using dimensionless quantities shown in relationship (3) [5].

$$\left(\frac{\partial^2}{\partial\rho^2}+\frac{1}{\rho}\frac{\partial}{\partial\rho}+\frac{1}{\rho^2}\frac{\partial^2}{\partial\theta^2}\right)\left(\frac{\partial^2\xi}{\partial\rho^2}+\frac{1}{\rho}\frac{\partial\xi}{\partial\rho}+\frac{1}{\rho^2}\frac{\partial^2\xi}{\partial\theta^2}\right)=0 \tag{3}$$

where: $\rho = r/b$; $\xi = w/h$ (Fig. 2).

In publications [4, 5] exploitative Clebsch assumption we can assume that solution of an equation (3) for loading according to fig. 2 is relationship (4) which determines plate deflection in its any point (e.g. point A – Fig. 2).

$$\begin{aligned}\xi = {} & A_0+B_0\rho^2+C_0\ln\rho+D_o\rho^2\ln\rho+A_1\rho+B_1\rho^3+C_1\rho^{-1}+D_1\rho\ln\rho \\ & +\sum_{m=2}^{\infty}\left[\left(A_m\rho^m+B_m\rho^{m+2}+C_m\rho^{-m}+D_m\rho^{2-m}\right)\cos(m\theta)\right]\end{aligned} \tag{4}$$

Moreover in publication [3] it was ascertained that solution determined by relationship (4) is sufficiently accurate if we take into consideration:

$$m_{max}=19 \tag{5}$$

Making in equation (4) substitution expressed by relationships (5), (6) and (7):

$$A_0+B_0\rho^2+C_0\ln\rho+D_o\rho^2\ln\rho=R_o \tag{6}$$

$$A_1\rho+B_1\rho^3+C_1\rho^{-1}+D_1\rho\ln\rho=R_1 \tag{7}$$

$$A_m\rho^m+B_m\rho^{m+2}+C_m\rho^{-m}+D_m\rho^{2-m}=R_m \tag{8}$$

and using condition (5) we obtain different form of relationship (4) determined by formula (8):

$$\xi=R_o+R_1+\sum_{m=2}^{19}R_m\left[\cos(m\theta)\right] \tag{9}$$

Constants occurred in relationships (4), (8) are determined basing on following boundary conditions of plate showing cut–off wheel model:

- in place of cut–off wheel fixing determined by press down discs circumference, for which: $\rho = \rho_i = a/b$

$$\xi = 0 \tag{10}$$

$$\frac{\partial \xi}{\partial \rho} = 0 \tag{11}$$

- on cut–off wheel circumference, on which $\rho = 1$:

$$M_r = 0 \tag{12}$$

where [2]:

$$M_r = -\frac{Dh}{b^2}\left[\frac{\partial^2 \xi}{\partial \rho^2} + \nu\left(\frac{1}{\rho}\frac{\partial \xi}{\partial \rho} + \frac{1}{\rho^2}\frac{\partial^2 \xi}{\partial \theta^2}\right)\right] \tag{13}$$

and after expansion in trigonometric series:

$$M_r = -\frac{Dh}{b^2}\sum_{m=0}^{19}\left\{\cos(m\theta)\left[R_m^{'''} + \nu\left(\rho^{-1}R_m^{'} - m^2\rho^{-2}R_m\right)\right]\right\} \tag{14}$$

- in place of force F action for elementary transverse force [4]:

$$Q_r = \frac{F}{2\pi b} \tag{15}$$

where:

$$Q_r = -\frac{Dh}{b^2}\left\{\frac{\partial}{\partial \rho}\left[\frac{1}{\rho}\frac{\partial}{\partial \rho}\left(\rho\frac{\partial \xi}{\partial \rho}\right) + \frac{1}{\rho^2}\frac{\partial^2 \xi}{\partial \theta^2}\right] + \frac{1-\nu}{\rho}\frac{\partial}{\partial \rho}\left(\frac{\partial^2 \xi}{\partial \theta}\right)\right\} \tag{16}$$

And after expansion in trigonometric series:

$$\begin{aligned} Q_r \quad = \quad & -\frac{Dh}{b^2}\sum_{m=0}^{19}\cos(m\theta)\left[R_m^{'''} + \rho^{-1}R_m^{''} - \rho^{-2}\left(1 + m^2(2-\nu)\right)R_m^{'}\right. \\ & \left. +\rho^{-3}(3-\nu)R_m\right] \end{aligned} \tag{17}$$

Using boundary conditions (10 – 15) for $m = 0$ we obtain system of equations (18 – 21).

$$A_0 + B_0\rho_i^2 + C_0\ln\rho_i + D_o\rho_i^2\ln\rho_i = 0 \tag{18}$$

$$2B_o\rho_i + C_o\rho_i^{-1} + D_o\rho_i(1 + 2\ln\rho_i) = 0 \tag{19}$$

$$2B_o(1+\nu) - C_o(1-\nu) + D_o(3+\nu) = 0 \tag{20}$$

$$D_o = -\frac{Fb^2}{8\pi Dh} \tag{21}$$

After substitution (in order to simplify further calculations) to system of equations (18 – 21):

$$\frac{Fb^2}{2\pi Dh} = K;\ A_o = a_o K;\ B_o = b_o K;\ C_o = c_o K;\ D_o = d_0 K \tag{22}$$

and solving such modified this system of equations with respect to new unknowns (new constants) a_o, b_o, c_o and d_o we obtain:

$$a_0 = -b_0\rho_i^2 - c_0 \ln\rho_i - d_o\rho_i^2 \ln\rho_i \tag{23}$$

$$b_o = \frac{c_o}{2}\frac{1-\nu}{1+\nu} + \frac{3+\nu}{8\,(1+\nu)} \tag{24}$$

$$c_o = \frac{\rho_i}{4}\frac{(1+2\ln\rho_i)\,(1+\nu) - (3+\nu)}{\rho_i^{-1}\,(1+\nu) + \rho_i\,(1-\nu)} \tag{25}$$

$$d_o = -\frac{1}{4} \tag{26}$$

Proceeding similarly we can calculate for $m = 1$ further unknowns, which display relationships:

$$a_1 = -b_1\rho_i^2 - c_1\rho_i^{-2} - d_1 \ln\rho_i \tag{27}$$

$$b_1 = -\frac{1+\nu+\rho_i^2\,(1-\nu)}{[(3+\nu)+\rho_i^4\,(1-\nu)]\,4} \tag{28}$$

$$c_1 = -\frac{b_1\,(3+\nu)}{1-\nu} - \frac{1+\nu}{4\,(1-\nu)} \tag{29}$$

$$d_1 = \frac{1}{2} \tag{30}$$

Proceeding similarly we can calculate for $m > 1$ next further unknowns, which display relationships:

$$d_m = -\frac{\left(1-\rho_i^2\right)(m-1) + \rho_i^{2m+2} + \frac{3+\nu}{1-\nu}}{C_1\left[\left(1-\rho_i^2\right)^2(m^2-1) + \left(\rho_i^{-2m+2} + \frac{3+\nu}{1-\nu}\right)\left(\rho_i^{2m+2} + \frac{3+\nu}{1-\nu}\right)\right]} \tag{31}$$

where $C_1 = m(m-1)(1-\nu)$

$$b_m = \frac{\left(1+\rho_i^2\right)(m+1) - \rho_i^{-2m+2} - \frac{3+\nu}{1-\nu}}{C_2\left[\left(1-\rho_i^2\right)^2(m^2-1) + \left(\rho_i^{-2m+2} + \frac{3+\nu}{1-\nu}\right)\left(\rho_i^{2m+2} + \frac{3+\nu}{1-\nu}\right)\right]} \tag{32}$$

where $C_2 = m\,(m+1)\,(1-\nu)$

$$a_m = -\frac{\rho_i^2}{m}\left[b_m\,(m+1) + d_m\rho_i^{-2m}\right] \tag{33}$$

$$c_m = \frac{\rho_i^2}{m}\left[\frac{b_m\rho_i^{2m}}{m} - d_m\,(m-1)\right] \tag{34}$$

According to relationship (23–34) calculated constants referring to cut–off wheel fixing, which for exemplary cut–off wheel is equal to $\rho = 1/3$ ($a = 50$ mm, $b = 150$ mm), have been collected in Tab. 1.

These constants can serve further for determination of:

Table 1 Constants values which determine cut–off wheel fixing ($\rho_i = 1/3$)

n	a	b	c	d
0	-0,17	0,300023926	0,099928222	-0,25
1	0,321613837	0,100384615	0,026538462	0,5
2	0,259480063	0,039581704	0,00310844	-0,056196247
3	0,097471578	-0,024496	0,000257041	-0,00347565
4	0,045140359	-0,01546767	1,96416E-05	-0,000235896
5	0,024966451	0,010400689	1,59651E-06	-1,79696E-05
6	0,015622076	0,007438821	1,37863E-07	-1,48939E-06
7	0,010628978	0,005580183	1,2442E-08	-1,30669E-07
8	0,007672964	0,004340259	1,15933E-09	-1,19264E-08
9	0,005787034	-0,00347222	1,10635E-10	-1,1203E-09
10	0,004513889	0,002840909	1,0754E-11	-1,07549E-10
11	0,003615702	0,002367424	1,06068E-12	-1,05014E-11
12	0,00295928	0,002003205	1,05861E-13	-1,03941E-12
13	0,002465483	0,001717033	1,0669E-14	-1,04027E-13
14	0,002084969	0,001488095	1,0841E-15	-1,05078E-14
15	0,001785714	0,001302083	1,10927E-16	-1,06968E-15
16	0,001546224	0,001148897	1,14183E-17	-1,09618E-16
17	0,001351644	0,001021242	1,18147E-18	-1,1298E-17
18	0,001191449	0,000913743	1,22806E-19	-1,17029E-18
19	0,001058018	0,000822368	1,28162E-20	-1,21756E-19

- cut–off wheel deflections in any selected its outside points of fixing ($1 > \rho > \rho_i$ i.e. $b > r > a$) according to formula (35), which determines dimensional value of cut–off wheel deflection after taking into consideration in formula (9) relationship (22) and earlier given relationship $\xi = w/h$.

$$\begin{aligned} w \quad = \quad & hK\{a_o + b_o\rho^2 + c_o \ln\rho + d_o\rho^2 \ln\rho \\ & +[a_1\rho + b_1\rho^2 + c_1\rho^{-1} + d_1\rho\ln\rho]\cos(\theta) \\ & + \sum_{m=2}^{19} [(a_m\rho^m + b_m\rho^{m+2} + c_m\rho^{-m} + d_m\rho^{-m+2})\cos(m\theta)]\} \end{aligned} \tag{35}$$

- elementary, radial bending moment in any selected points of cut–off wheel in place of its fixing and outside of it ($1 > \rho \geq \rho_i$ i.e. $b¿r \geq a$) according to formula (36), which results from formula (14) after performing in it designed

differential operations;

$$M_r = \frac{F}{2\pi}\{-2b_o\,(1+\nu) + c_o\rho^{-2}\,(1-\nu) - d_o\,[3+\nu+2\,(1+\nu)\ln\rho]$$

$$+\left[-b_1\,(3+\nu)\,\rho - 2c_1\,(1-\nu)\,\rho^{-3} - d_1\,(1+\nu)\,\rho^{-1}\right]\cos\left(\theta\right)$$

$$+\sum_{m=2}^{19}[\,-a_m m\,(m-1)\,(1+\nu)\,\rho^{m-2} - b_m\,(m+1)\,(m+2-\nu\,(m-2))\,\rho^m$$

$$-c_m m\,(m+1)\,(1-\nu)\,\rho^{-m-2}$$

$$-d_m\,(m-1)\,(m-2-\nu\,(m+2))\,\rho^{-m}]\cos(m\theta)\} \tag{36}$$

- elementary, circumferential bending moment in any selected points of cut–off wheel in place of its fixing and outside of it ($1 > \rho \geq \rho_i$ i.e. $b > r \geq a$) according to formula (39), which results from formula (37) [2] and its expansion in trigonometric series (38) after performing in it designed differential operations.

$$M_\theta = -\frac{Dh}{b^2}\left[\nu\frac{\partial^2\xi}{\partial\rho^2} + \left(\frac{1}{\rho}\frac{\partial\xi}{\partial\rho} + \frac{1}{\rho^2}\frac{\partial^2\xi}{\partial\theta^2}\right)\right] \tag{37}$$

$$M_\theta = -\frac{Dh}{b^2}\sum_{m=0}^{19}\left\{\cos\left(m\theta\right)\left[\nu R_m^{''} + \left(\rho^{-1}R_m^{'} + m^2\rho^{-2}R_m\right)\right]\right\} \tag{38}$$

$$M_\theta = \frac{F}{2\pi}\{-2b_o\,(1+\nu) - c_o\rho^{-2}\,(1-\nu) - d_o(1+2\ln\rho+\nu\,(3+2\ln\rho))$$

$$+\left[2b_1\rho\,(3\nu+1) + 2c_1\rho^{-3}\,(\nu-1) + d_1\rho^{-1}\,(1+\nu)\right]\cos\theta$$

$$+\sum_{m=2}^{19}[a_m\rho^{m-2}m(m-1)(\nu-1) + b_m\rho^m((m+2)(m+1)\nu + m + 2 - n^2)$$

$$+c_m\rho^{-m-2}m(m+1)(\nu-1) \tag{39}$$

$$+d_m\rho^{-m}(\nu(2-m)(1-m) + 2 - m - m^2)]\cos(m\theta)\}$$

According to calculated formulas (36) and (39) moments enable determination of radial and circumferential tensile stresses on surface of accepted cut–off wheel model suitably according to relationship (40) and (41)

$$\sigma_r = \frac{6M_r}{h^2} \tag{40}$$

$$\sigma_\theta = \frac{6M_\theta}{h^2} \tag{41}$$

and finally reduced stresses according to relationship (42).

$$\sigma = \sqrt{(\sigma_r^2 + \sigma_\theta^2)} \tag{42}$$

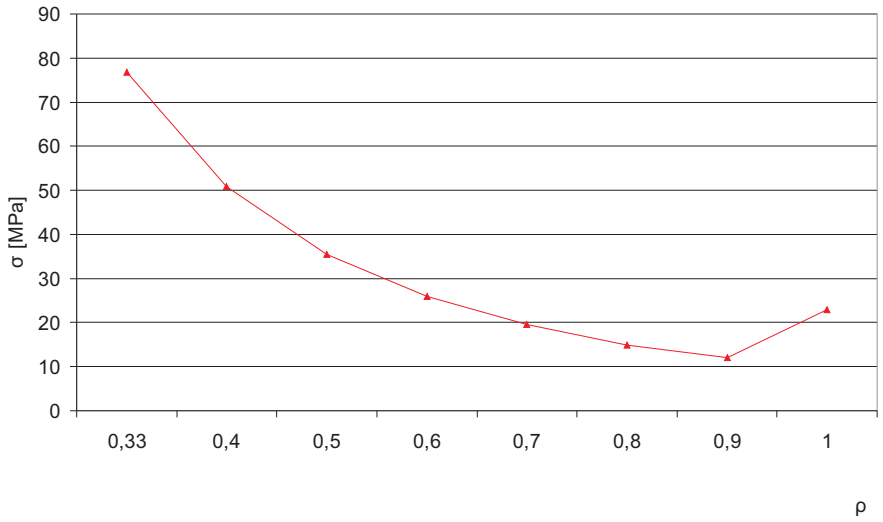

Figure 3 Stresses distribution in cut–off wheel model in plane of action of force F determined by analytic method

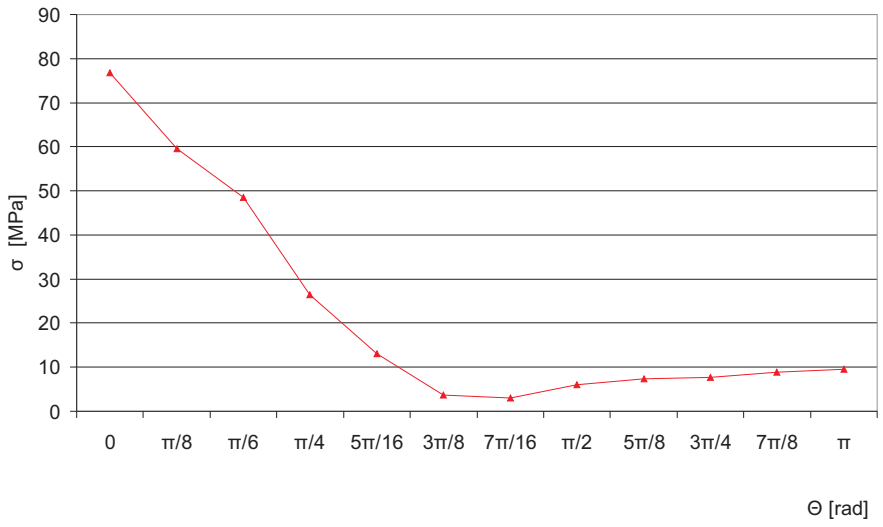

Figure 4 Stresses distribution in cut–off wheel model across half–circumference of cut–off wheel fixing determined by analytic method

Calculations of constants a, b, c, d and M_r, M_θ, σ_r i σ_θ have been done using *Microsoft Excel* program and the correctness of these computations have been confirmed using *Mathematica 7.0 program.* For previously determined [2] value of

material properties of exemplary cut–off wheel *41-300x3, 0x32 95A24RBF-100:* $\nu = 0,202$, $E = 29783$ MPa and force value $F = 100$ N, distributions of values of considered quantities have been presented on diagrams: $\sigma(\rho)$ – Fig. 3 and $\sigma(\theta)$ – Fig. 4. Maximal reduced stresses, calculated according to formula (39) occur in intersection point of cut–off wheel fixing circle by plane of action of force F and crossing simultaneously through cut–off wheel axis. They are equal to: $\sigma_{max} = 76,8$ MPa.

1. **Stresses determination in accepted cut–off wheel model using FEM method**

FEM method has been applied for strengh estimation of cut–off wheel using *Ansys 12.1* program with element section of fractional type of the order of 2 with 5 degrees of freedom typical for thin-walled circular plates section.

Obtained diagrams of considered above values have been shown in Fig. 5 and Fig. 6, however visualization of stresses distribution in whole cut–off wheel has been depicted in Fig. 7. Values of reduced stresses in this method has been equel to $\sigma_{max} = 52,8$ MPa.

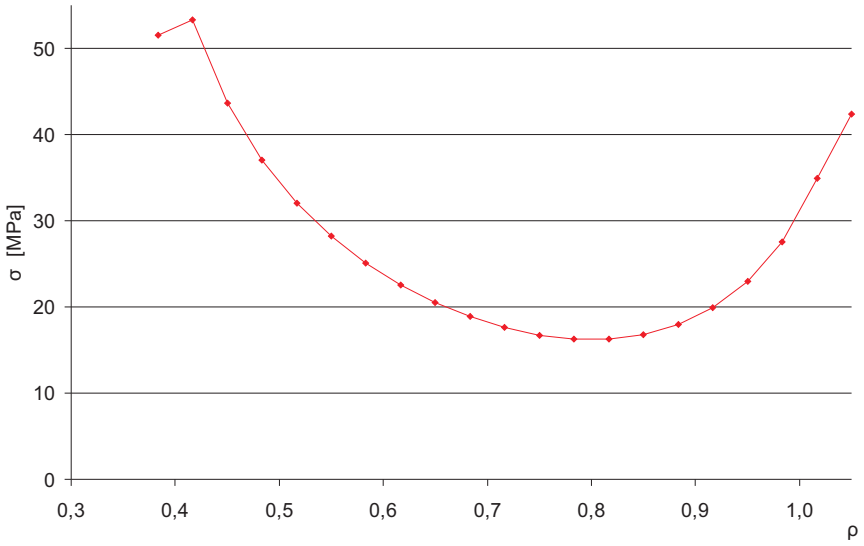

Figure 5 Stresses distribution in cut–off wheel model in plane of action of force F determined by FEM method

4. Stresses determination in cut–off wheel by strain gauge method

The practical estimation of cut–off wheel strength has been carried out by strain gauge method using investigation stand which has been already shown earlier [2]. Three cut–off whells of idential technical characteristic and manufactured in the

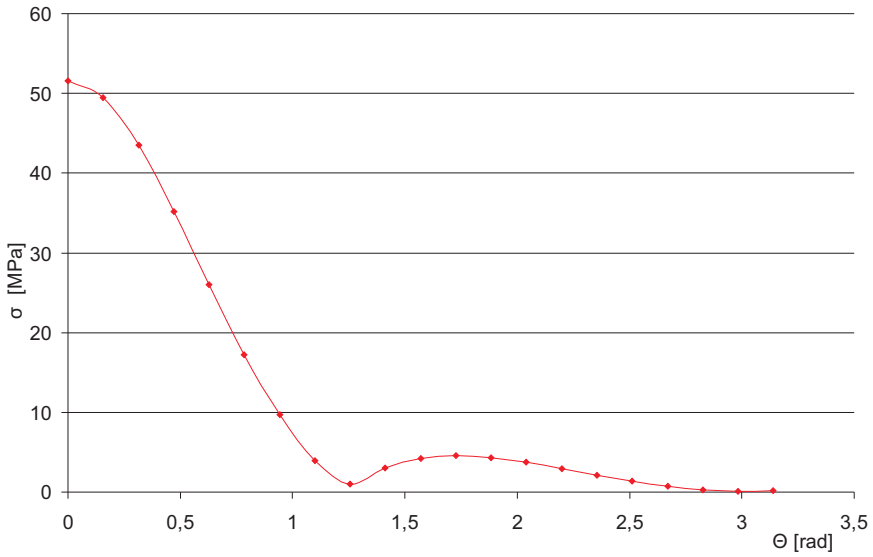

Figure 6 Stresses distribution in cut–off wheel model across half–circumference of cut–off wheel fixing determined by FEM method

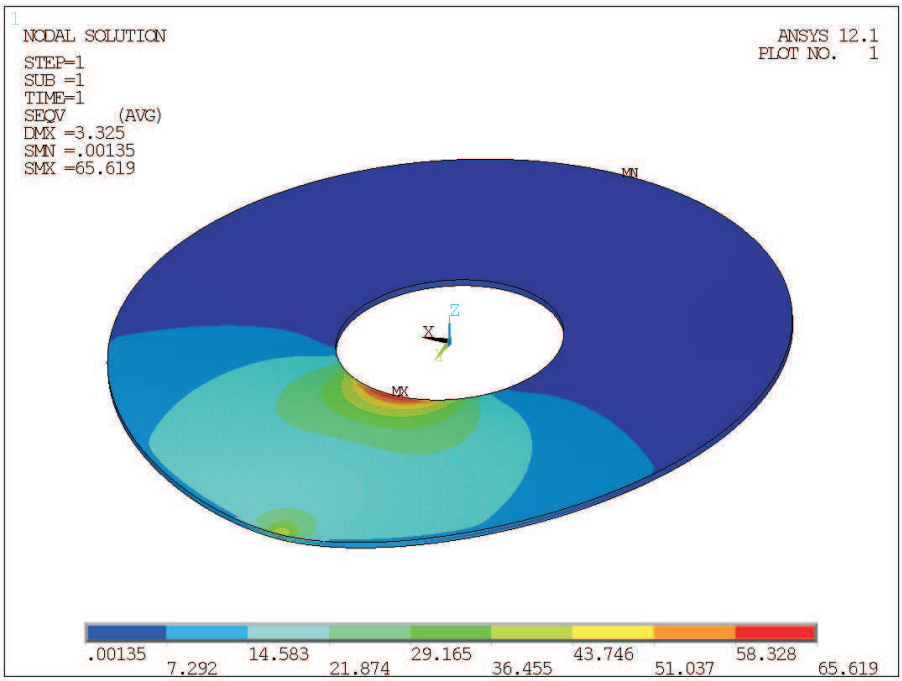

Figure 7 Stresses distribution in cut–off wheel model determined by FEM method

same production lot have been investigated. Samples for determination of Poisson ratio and Young's modulus necessary for determination of stresses in all considered methods have been also taken from the same lot of biaxial strain gauge of *TX-5-2x* type have been used for investigation of each cut–off wheels from which signal has been transferred to amplifier *Spider 8* controlled by *Catman Easy* program. Strain gauge have been located in place maximal stresses occurance. Each cut–off wheel has been loaded in place of its circumference by lateral force of value$F$= 100N. From readed from slotted section values of reduced stresses we have calculated average values which have been equel to $\sigma_{max} = 58,9$ MPa.

5. Investigation results obtained in cautious methods of estimation of cut–off wheel model strength

Results obtained in three shown above methods of reduced stresses values estimation occurred in cut–off wheel model have been shown in table 2.

Table 2 Stresses values σ_{max} [MPa] in cut–off wheel model and in cut–off wheel obtained in considered estimation methods

Methods of cut–off wheel strength estimation		
analytical	FEM	strain gauge
76,8	52,8	58, 9

6. Summary

The investigation results are obtained in the work considered, methods of stress determination in circular plates as cut–off wheel models are different.

In the analytical method application of the accepted trigonometric series as a solution of an equation of circular symmetric plate deflection as the cut–off wheel model is doubtful. The occurrence of stresses of high values (about 9,5 MPa) on the contrary side of the imposed force (right end of diagram in Fig. 4) give evidence of this fact. These stresses are close to zero in FEM method (right end of diagram in Fig. 6) and in extensometrical method. It follows that the results obtained in the analytical method are overvalued. Moreover, this method is very labour-intensive despite computer support for calculations. Also labour–intensive is the strain gauge method, which needs special preparation (offset surface) of the cut–off wheel, which may disturb obtained stress values.

The least labour–intensive from the considered methods is the FEM method using *ANSYS 12.1* program , but it generates certain problems with modeling at a place of impose of the force (considerable stresses occurred at the place of impose of the force – right end of diagram in Fig. 5). This place is also difficult to determine experimentally). Despite of this fact this method can be acknowledged as the most reliable. It is shown, for example, by a decrease of stress values next to the circuit under the fixing plates of the cut–off wheel (right end of diagram in Fig. 5). Moreover, this method found approval and is widely applied for determination of stresses in many constructions of different complexity degrees.

References

[1] **Kaczmarek J.**: Wytrzymałość statyczna ściernic do przecinania, *XXX Naukowa Szkoła Obróbki Ściernej*, Rzeszów, **2007**.

[2] **Kaczmarek J.**: Badania wytrzymałości ściernic metodą tensometryczną, *XXXI Naukowa Szkoła Obróbki Ściernej*, Rzeszów, **2008**.

[3] **Niezgodziński M.E. and Niezgodziński T.**: Wzory wykresy i tablice wytrzymałościowe, *WNT Warszawa*, p.143, **1996**.

[4] **Rejssner H.**: Über die unsymmetrische Biegung dünner Kreisringplaten.

[5] **Timoschenko S., Woinowski–Krieger S.**: Teoria płyt i powłok, *Arkady*, **1962**.

[6] Sprawozdanie z realizacji projektu badawczego nr 4 T07D 010 29: System wielokryterialnej oceny i doskonalenia wytrzymałości ściernic do przecinania, Łódź, **2008**.